*Acta metall.* Vol. 36, No. 8, pp. 2239–2248, 1988
Printed in Great Britain. 

0001-6160/88 $3.00 + 0.00


# A NOVEL VIEWPOINT ON THE Cu–Au PHASE DIAGRAM: THE INTERPLAY BETWEEN FIXED ISING ENERGIES AND ELASTIC EFFECTS

**A. ZUNGER, S.-H. WEI, A. A. MBAYE and L. G. FERREIRA**
Solar Energy Research Institute, Golden, CO 80401, U.S.A.

(*Received* 20 *June* 1987; *in revised form* 16 *November* 1987)

**Abstract**—Theoretical models of temperature-composition phase diagrams of binary A–B systems have traditionally been based on various approximate solutions to the same broad class of physical Hamiltonian—the generalized Ising model. Common to all such approaches is the description of the interaction energies between sites, pairs or multi-atom clusters of A and B by some *fixed* (volume-independent) parameters. Despite extensive attempts to improve on the *method* of solution to the statistical problem (quasi chemical approach, cluster variation method i.e. CVM, high-temperature expansions, Monte Carlo), or to increase the *range* of the interaction to further neighbors, numerous *qualitative* discrepancies with real phase diagrams (briefly reviewed here) remain. We show that the source of the difficulty is not in the satistical method or range of interaction, but rather in the physical content of the interaction energies used. Recognizing that all successful classical packing models of solids require a description of the *competition* between fixed-volume "chemical" energies (representable as fixed Ising interaction parameters) and size-mismatch "elastic" energies (not representable by fixed energies), we include both on the same footings in a generalized Ising-like approach. Calculating both terms from first-principles self-consistent band theory we show through CVM calculations on the prototype Cu–Au phase diagram how many of the deficienciesof the "chemical-only" Ising models can be cured. This reveals the dominant role of lattice relaxation in determining many of the thermodynamic properties and the phase diagram.

**Résumé**—Les modèles théoriques des diagrammes de phases température-composition pour les systèmes binaires A–B ont été basés traditionnellement sur diverses solutions approchées appartenant à la même et vaste classe d'hamiltoniens physiques, le modèle d'Ising généralisé. Le point commun à toutes ces approches est la description des énergies d'interaction entre sites, entre paires ou entre amas multi-atomiques des éléments A et B par des paramètres *fixes* (indépendants du volume). Malgré de nombreux essais pour améliorer le *mode* de solution du problème statistique (approche quasi-chimique, méthode de la variation des amas, développements à haute température, Monte Carlo), ou pour étendre le *domaine* d'interaction aux seconds voisins, il demeure de nombreux désaccords *qualitatifs* avec les diagrammes de phases réels (nous en présentons ici une revue rapide). Nous montrons que la source des difficultés n'est pas dans la méthode statistique ou dans le domaine d'interaction, mais qu'elle réside plutôt dans le contenu des énergies d'interaction que l'on utilise. Reconnaissant que tous les modèles classiques d'empilement valables pour les solides nécessitent une description de la *compétition* entre les énergies "chimiques" à volume fixe (que l'on peut représenter par des paramètres fixes d'interaction d'Ising) et les énergies "élastiques" de désaccord de taille (que l'on ne peut décrire par des énergies fixes), nous tenons compte également de ces deux types d'énergie dans une approche généralisée qui ressemble au modèle d'Ising. En calculant les deux termes à partir d'une théorie des bandes auto-cohérente basée sur les premiers principes, nous montrons—à l'aide de calculs réalisés par la méthode de la variation des amas, dans le cas du diagramme de phases modèle Cu–Au—comment l'on peut remédier aux défauts des modèles d'Ising qui ne sont basés que sur l'aspect chimique. Ceci révèle le rôle dominant de la relaxation du réseau pour déterminer de nombreuses propriétés thermodynamiques ainsi que le diagramme de phases.

**Zusammenfassung**—Theoretische Modelle von Phasendiagrammen (Zusammensetzung/Temperatur) binärer A–B-Systeme werden traditionell aufgebaut auf verschiedenen Näherungslösungen derselben breiten Klasse von Hamilton-Gleichungen—dem verallgemeinerten Isingmodell. Alle diese Näherungen haben die Beschreibung der Wechselwirkungsenergien zwischen Gitterplätzen, Paaren oder Multiatom-clustern von A- und B-Atomen durch einige *feste* (volumunabhängige) Parameter gemeinsam. Trotz ausführlicher Versuche, die Lösungs*methode* des statistischen Problems (quasichemische Näherung, Clustervariationsmethode, Hochtemperaturenäherungen, Monte-Carlo) zu verbessern oder den *Bereich* der Wechselwirkung zu weiteren Nachbarn zu vergrößern, bleiben doch viele *qualitative* Diskrepanzen zu den (hier kurz dargestellten) realen Phasendiagrammen. Wir zeigen, daß die Ursache der Schwierigkeit nicht in der statistischen Methode oder im Bereich der Wechselwirkung liegt, sondern vielmehr in der physikalischen Bedeutung der benutzten Wechselwirkungsenergien. Aus der Erkenntnis heraus, daß alle erfolgreichen klassischen Packungsmodelle der Festkörper eine Beschreibung der *Konkurrenz* zwischen "chemischen" Energien bei festem Volumen (darstellbar als feste Ising-Wechselwirkungsparameter) und "elastischen" Energien wegen Größenfehlpassung (nicht darstellbar durch feste Energien) erfordern, schließen wir beide auf derselben Grundlage in eine verallgemeinerte Ising-artige Näherung ein. Mit der Berechnung beider Terme auf der Grundlage der selbst-konsistenten Bandtheorie zeigen wir mit Berechnungen mittels der Clustervariationsmethode zum Prototyp des Phasendiagrammes, Cu–Au, wie viele der Unstimmigkeiten der "nurchemischen" Isingmodelle ausgeräumt werden können. Dieses Vorgehen enthüllt die wesentliche Rolle der Gitterrelaxation bei der Bestimmung der thermodynamischen Eigenschaften und des Phasendiagrammes.

## 1. INTRODUCTION: THE ISING APPROACH TO ALLOY PHASE DIAGRAMS AND THE COUNTING-STATISTICS PROBLEM

### *1.1. Statement of the problem*

The great diversity of structural phenomena exhibited by a binary $A_xB_{1-x}$ alloy of constituents A and B as a function of composition $x$ and temperature $T$ (order, disorder, miscibility gaps, spinodal decomposition, multiple-phase coexistence, etc.) has traditionally been analyzed through generalized nearest-neighbor Ising models with the interaction Hamiltonian of the type [1–4]

$$\hat{H} = J_0 N + J_1 \sum S_i + J_2 \sum S_i S_j + J_3 \sum S_i S_j S_k + J_4 \sum S_i S_j S_k S_l + \cdots, \quad (1)$$

where $N$ is the number of sites, each occupied either by A ("spin up") or by B ("spin down"), $S$ are the spin variables, and $J_h$ is the $h$-site interaction energy. Each of the distinct $2^N$ possible arrangements on the lattice is a "state of order" denoted $\sigma$. For f.c.c. lattices one has $6N$ pairs, $8N$ triplets (equilateral triangles) and $2N$ quadruplets (tetrahedra). It has been customary [4, 5] to express $\hat{H}$ in f.c.c. systems in terms of five tetrahedra, each having a concentration $N_n$ and the composition $A_{4-n}B_n$ ($0 \leqslant n \leqslant 4$, where $n = 0$ and $n = 4$ denote the end-point constituents $A_4$ and $B_4$, respectively), as

$$\hat{H} = \sum_{n=0}^{4} E_n N_n, \quad (2)$$

where

$$\sum_n N_n = 2N,$$

and where $E_n$ is the energy of tetrahedron of type $n$. Comparison of equations (1) and (2) shows that since each site is shared by eight tetrahedra and each pair is shared by two tetrahedra, the mapping between the multisite energies $J_h$ and the tetrahedron energies $E_n$ is [5]

$$\begin{aligned}
E_0 &= \tfrac{1}{2}J_0 - \tfrac{1}{2}J_1 + 3J_2 - 4J_3 + J_4 \quad \text{for } A_4;\\
E_1 &= \tfrac{1}{2}J_0 - \tfrac{1}{4}J_1 + 0 + 2J_3 - J_4 \quad \text{for } A_3B;\\
E_2 &= \tfrac{1}{2}J_0 + 0 - J_2 + 0 + J_4 \quad \text{for } A_2B_2;\\
E_3 &= \tfrac{1}{2}J_0 + \tfrac{1}{4}J_1 + 0 - 2J_3 - J_4 \quad \text{for } AB_3;\\
E_4 &= \tfrac{1}{2}J_0 + \tfrac{1}{2}J_1 + 3J_2 + 4J_3 + J_4 \quad \text{for } B_4. \quad (3)
\end{aligned}$$

To fix the reference energy, one follows the conventional definition of *excess* thermodynamic functions (enthalpy, entropy) and defines the excess energy per atom $\Delta E(n)$ of tetrahedron $A_{4-n}B_n$ with respect to equivalent amounts of its constituent solids A and B at equilibrium as

$$\Delta E(n) = \tfrac{1}{4}E_n[A_nB_{4-n}] - \frac{4-n}{4}E_0[A] - \frac{n}{4}E_4[B]. \quad (4)$$

From equations (3) and (4) one has

$$\begin{aligned}
\Delta E(0) &= 0;\\
\Delta E(1) &= -3J_2 + 4J_3 - 2J_4;\\
\Delta E(2) &= -4J_2 \equiv 2\omega;\\
\Delta E(3) &= -3J_2 - 4J_3 - 2J_4;\\
\Delta E(4) &= 0; \quad (5)
\end{aligned}$$

where $J_0$ and $J_1$ do not appear, and where $J_3$ is the only distinguishing interaction term between $n = 1$ and $n = 3$. Defining the occupation variables $\eta_1^{(i)} = 1$ and $\eta_0^{(i)} = 0$ for occupation of site $i$ by atom B [where $S^{(i)} = 1$] and $\eta_1^{(i)} = 0$, $\eta_0^{(i)} = 1$ for occupation by A [where $S^{(i)} = -1$], one has

$$\eta_1^{(i)} - \eta_0^{(i)} = S^{(i)}, \qquad \eta_1^{(i)} + \eta_0^{(i)} = 1. \quad (6)$$

The multi-site correlation functions $\xi_n(\sigma)$ for the state of order $\sigma$ are then

$$\xi_n(\sigma) = \frac{1}{N_4}\sum_t \eta_p^{(i)}\eta_q^{(j)}\eta_r^{(k)}\eta_s^{(l)}, \quad (7)$$

where $t$ denotes sum over the $N_4$ tetrahedra whose four sites are $p$, $q$, $r$ and $s$. The excess energy of the A–B system in a state of order $\sigma$ is then

$$\Delta E(\sigma) = \sum_n \Delta E(n)\xi_n(\sigma). \quad (8)$$

The well-known single-site (Bragg–Williams) approximation refers to the choice $J_2 = J_3 = J_4 = 0$, whereas (Bethe's) pair approximation corresponds to $J_3 = J_4 = 0$. In the latter case, one has from (5)

$$\Delta E(1) = \Delta E(3) = \tfrac{3}{4}\Delta E(2) = \tfrac{3}{2}\omega \quad \text{(pairwise additive).} \quad (9)$$

Generalization of (9) to multi-site interactions can be done by defining the non-pairwise (dimensionless) parameters $\alpha$ and $\beta$ from

$$\begin{aligned}
\Delta E(1) &\equiv \tfrac{3}{4}\Delta E(2)(1+\alpha) \equiv \tfrac{3}{2}\omega(1+\alpha),\\
\Delta E(3) &\equiv \tfrac{3}{4}\Delta E(2)(1+\beta) \equiv \tfrac{3}{2}\omega(1+\beta), \quad (10)
\end{aligned}$$

where $\alpha = \beta = 0$ corresponds to the pair approximation, and where $\omega$ is the "pair interaction parameter" [1, 2].

### *1.2. The traditional source of difficulty*

Modeling alloy phase diagrams by equations (1)–(10) requires the specification of the energies and a method for determining the entropy of each phase. The first problem was circumvented early on by identifying $\{J_h\}$ or $\Delta E(n)$ with some fixed, short range interactions, analogous in spirit to those used in the original application of (1) to magnetism [1]. The main effort focused then on the statistical methods of solution of equation (1).

The source of difficulty there has been that both the excess energy [equation (8)] and the entropy depend on the complete set $\{\xi(\sigma)\}$ of correlation functions (hence, the partition function) for which no exact solution exists in three dimensions. Many of the approximate methods of solutions are based on counting algorithms for the number of distinct

configurations of the crystal that can be constructed from packing a given "cluster" of sites. The size of the cluster and hence the number of possible modes of occupancy of *its* sites define a "topological counting range", not to be confused with the "interaction range" within which $h$ atoms are *physically* coupled through a potential $J_h$. (Often, but not always, the "topological counting range" is set to be equal to the "interaction range".) Different approximations to the evaluation of the entropy are distinguished by using different topological counting ranges and by the various ways in which one attempts to correct for conflicting occupancies of two or more adjoining clusters (e.g. a configuration in which some sites occur simultaneously in a A–A *and* a B–B pair is conflicting). Since inclusion of conflicting configurations spuriously stabilizes ordered phases over disordered phases, it *overestimates* the critical order–disorder temperature $T_c$.

Various applications of the generalized Ising model to calculate the phase diagram of the classical test case—the all-f.c.c. Cu–Au system—are hence distinguished by the choice of (i) the physical interaction range (i.e. the numer of $J$s) retained (First nearest neighbors, second nearest neighbors, retention in the first nearest neighbor model of single sites; pairs, etc.), (ii) the topological counting range (pair, tetrahedron, tetrahedron–octahedron, etc.) and (iii) the algorithm used to calculate the entropy (or correlation functions) within a prescribed topological counting range (MC, CVM, etc.).

Early application by Shockley [6] of the Bragg–Williams technique [7] (points only for both topological and interaction ranges) to the Cu–Au system revealed a phase diagram which fails to separate the distinct $Cu_3Au \leftrightarrows Cu_{0.75}Au_{0.25}$ and the $CuAu_3 \rightleftarrows Cu_{0.25}Au_{0.75}$ order–disorder transitions from that of $CuAu \rightleftarrows Cu_{0.5}Au_{0.5}$, described the latter erroneously as a *second* order transition, and in the case of ferromagnetic interactions the phase separation critical temperature was $kT_c/12J_2 = 1.0$. This approach produced a symmetry of the phase diagram about $x = 0.5$, unlike the data. Bethe's [8] use of a site-only interaction range but including pairs in the topological counting range and an improved counting algorithm (equivalent to the quasi-chemical approach [9]) produced similar results with the exception of the survival of some short range order in the disordered phase, and that the phase separation critical temperature $kT_c/12J_2$ was lower (0.9142). Li's [10] extension of the topological counting range to a tetrahedron (retaining pairs-only in the physical interaction range), produced for the first time a separation of all three distinct order–disorder transitions, but retained the unphysical feature of symmetry about $x = 0.5$ and the absence of joined (two-phase) regions between the three ordered phases. It has then been realized [4, 11–14] that the inherent deficiency of the pairs-only topological counting range to f.c.c. structures is its inability to describe frustration effects: since these structures exhibit both triangles and tetrahedra and since these units cannot accommodate only unlike adjacent atoms, the system is frustrated at the presence of attractive A–B interactions. Higher order (e.g. four-body) interactions are then required to represent a reasonable energy compromise. Increasing the topological counting range to a tetrahedron (by Van Baal [12], Kikuchi [13], Golosov *et al.* [14]) or tetrahedron–octahedron [15], yet retaining the pairs-only physical interaction range ($J_2$) has showed a rather fast convergence of the phase diagram with respect to the counting statistics, revealing the three separate order–disorder transitions and the two-phase coexistence regions, [2, 4] and in the case of ferromagnetic interaction the phase separation critical temperature was $kT_c/12J_2 = 0.835$ for tetrahedron topology (which we use), $kT_c/12J_2 = 0.834$ for tetrahedron–octahedron topology, compared with the accurate high-temperature expansion result of $kT_c/12J_2 = 0.816$ (see [4, 16]). While unlike the observed phase diagram [17], the one obtained with pair-only physical interactions ($J_2$) was still symmetric at $x = 0.5$, it was quickly realized [12] that the desired asymmetry could be reproduced by introducing a nonzero $J_3$ [see equation (5) where $J_3 \neq 0$ makes $\Delta E(1) \neq \Delta E(3)$], or equivalently, using nonzero $\alpha$ and $\beta$ in equation (10). The best agreement with the observed phase diagram of Cu–Au was obtained [18] by fitting the three observed critical temperatures by adjusting in equation (10) $\{\omega, \alpha, \beta\}$.

### *1.3. The real difficulty: the physical content of the interaction energies*

This problem lay dormant for a few years, until it has recently been realized [20–21] that the real difficulty in representing actual phase diagrams through eqauation (1) lies in the physical content and interpretation of the excess cluster energies $\{\Delta E(n)\}$ or, equivalently the coupling constants $\{J_n\}$. While in the magnetic analog of the alloy problem there was generally no reason to believe that the interaction energies $J$ depend on the magnetization, in the actual alloy problem, the physical interactions could depend on composition $x$, or, alternatively, on the molar volume $V(x)$. In general, the two end-point elemental solids A and B can have different molar volumes ($V_A$ and $V_B$, respectively), hence the solid alloy has $V(x) \neq V_A \neq V_B$. Consequently, $\Delta E(n)$ of equation (4) is a *function* of volume:

$$\Delta E(n, V) = \tfrac{1}{4}E_n[A_nB_{4-n}, V] - \frac{4-n}{4}E_0[A, V_A] - \frac{n}{4}E_4[B, V_B]. \quad (11)$$

While the role of elastic energies was recognized early on [22], its detailed effects on the features of the phase diagram [or its simple separable form noted in equations (15)–(20) below] were not generally appreciated. The physical content of $\Delta E(n, V)$ can be appreciated

by considering the special state of order $\sigma$ where all of the $N_4$ tetrahedra have the same occupation number $n$, hence $\xi_m(n)$ of equation (7) is just $\delta_{nm}$. This corresponds to an ordered crystal (e.g. $L1_0$, or $L1_2$) whose repeat unit is a given (fixed) tetrahedron $A_{4-n}B_n$. The volume-dependent energy $E_n[A_nB_{4-n}, V]$ is then simply the $(T=0)$ equation of state of this solid, and the value of $\Delta E(n, V)$ of equation (11) at the *equilibrium* volume $V_n$ [which minimizes $E_n(V)$] is the formation enthalpy of this ordered phase from its constituent elemental solids, i.e.

$$\Delta H^{(n)} \equiv \Delta E(n, V_n) \tag{12a}$$

or,

$$\Delta H^{(n)} \equiv E^{(n)}[A_nB_{4-n}] - nE[A] - (4-n)E[B]. \tag{12b}$$

Clearly, from equations (11) and (12)

$$\Delta E(n, V) = \Delta H^{(n)} + F(V - V_n) \tag{13}$$

where $F$ is a general (harmonic or anharmonic) positive function.

The physical content of equation (13) can be further appreciated by considering the formation of an ordered structure $A_{M-m}B_m$ with $N_A$ A atoms and $N_B$ B atoms ($N = N_A + N_B$ in total) from the constituent solids in two formal steps. *First*, compress or dilate the pure crystals $A_{M-m}A_m$ from its equilibrium volume $V_A$ to the volume $V$ akin to the final structure ($A_{M-m}B_m$): do the same for pure $B_{M-m}B_m$, changing its volume from $V_B$ to $V$. Clearly, since in both cases deformation of *equilibrium* structures is involved, this step requires the *investment* of some elastic energy

$$\Delta F[N_A, N_B, V] = \frac{N_A}{N}\{E_0[A, V] - E_0[A, V_A]\} + \frac{N_B}{N}\{E_4[B, V] - E_4[B, V_B]\}. \tag{14}$$

*Second*, using these "prepared" fixed lattices, "flip" the necessary number of A atoms in $A_{M-m}A_m$ into B and similarly "flip" B atoms in $B_{M-m}B_m$ into A to create the desired structure $A_{M-m}B_m$. Since A is different chemically from B, this step might involve the (release or absorption) of a "substitution" or "chemical" energy $\epsilon^{(m)}$ associated with chemical events between A and B (e.g. charge transfer, Madelung energies, bond formation, exchange interactions, etc.). The total energy change associated with the chemical reaction $N_A A + N_B B \rightarrow A_{N_A}B_{N_B}$ is hence the sum of the energies of the two steps, or

$$\Delta E(m, V) = \epsilon^{(m)} + \Delta F[N_A, N_B, V]. \tag{15}$$

From equations (12), (13) and (15) one observes that

$$\Delta H^{(m)} \equiv \epsilon^{(m)} + \Delta F[N_A, N_B, V^{(m)}] \tag{16}$$

i.e. as recognized by numerous classical models of crystal packing [23–25] and phase stability [25–28], the low-temperature stability (or even existence) of a crystal represents, among others, the consequence of a *competition* between volume-dependent destabilizing elastic energies $\Delta F$ associated with packing of components of different sizes, and the potential stabilization associated with "chemical" (often termed also "electrochemical", or "electronic") interactions, $\epsilon$.

Ferreira *et al.* [21] have recently shown that when the molar volume $V$ at a fixed composition does not depend on the state of order $\sigma$, then $\Delta F$ of equation (15) can be rigorously expressed in terms of the bulk modulus $B(x)$ and equilibrium volume $V(x)$ as

$$\Delta F = (1 - X_n)\int_0^{X(V)} xZ(x)\,dx + X_n\int_{X(V)}^1 (1-x)Z(x)\,dx \equiv G(X_n), \tag{17}$$

where

$$Z(x) = \frac{B(x)}{V(x)}\left(\frac{dV}{dx}\right)^2 = -\frac{d^2G}{dx^2} \tag{18}$$

and $X_n$ is the concentration of the B atom in $A_{4-n}B_n$. More generally, using (8),

$$E(\sigma, V) = \sum_n \epsilon^{(n)}\xi_n(\sigma) + G(x), \tag{19}$$

where

$$G(x) = (1-x)\int_0^x x'Z(x')\,dx' + x\int_x^1 (1-x')Z(x')\,dx'. \tag{20}$$

Hence, given $\{\Delta H^{(n)}, B(x), V(x)\}$ one can calculate from (17)–(20) the quantities $\{\epsilon^{(n)}, G(x)\}$ which completely define within this ("$\epsilon$–$G$") approach the interaction Hamiltonian in the presence of both "chemical" ($\epsilon$) and "elastic" ($G$) energies.

The configuration average of $\Delta E(\sigma, V)$ taken for the disordered (D) phase gives the mixing enthalpy of $A_xB_{1-x}$ i.e.

$$\Delta H^{(D)}(x, T) \equiv H^{(D)}[A_xB_{1-x}] - xH[A] - (1-x)H[B].$$

The point we wish to make is that previous applications of Ising-like models [equation (1)] to alloy phase diagrams have interpreted the $J_n$s or, equivalently the $\Delta E(n)$s [equations (5) and (8)–(10)] as *energies on a fixed lattice*, corresponding hence to $\epsilon^{(m)}$ of (15), and neglecting the elastic energies $\Delta F$ associated with the atomic size mismatch between the constituents. While cures to various failures of such models in describing actual phase diagrams were traditionally sought through improvements in the counting statistics beyond the tetrahedron topology (using, for example, tetrahedron–octahedron CVM [4], Monte-Carlo [19], high-temperature expansions, e.g. [1, 2, 4]), it is surprising that the role of atomic size mismatch–the single most important feature of all classical models of packing of atoms of different

sizes in solids [23–28]—was largely neglected in phase diagram calculations. In what follows, we describe the shortcomings of such traditional nearest-neighbor Ising approaches which are associated with the neglect of elastic effects (Section 2) and then offer a cure (Section 3). Application to the calculation of phase diagram of Cu–Au then follow (Sections 3.1–3.3).

## 2. QUALITATIVE EFFECTS OF THE ELASTIC ENERGY

First note that equations (15) [or (19)] show which phenomena *do not* depend on the elastic term: to the extent that order–disorder transformations at a fixed composition involve but a negligible change in volume (hence, elastic energy), the energy $\Delta F[N_A, N_B, V]$ of equation (15) [or $G(x)$ of (19)] is common to both the ordered and the disordered phase, hence by (19) only $\Sigma\xi_n(\sigma)\epsilon^{(n)}$ distinguishes them. Order–disorder transition temperatures would then depend almost entirly on $\{\epsilon^{(n)}\}$, terms which were treated adequately by conventional Ising models of alloys [1, 2, 4–16]. In contrast, $G(x)$ makes its presence known in *multiple-phase phenomena*: consider, for example, the coexistence of two phases at equilibrium with concentrations $x_1$ and $x_2$ ($x_1 \neq x_2$). Since in general $G(x_1) \neq G(x_2)$, the inclusion of $G(x)$ in $\Delta E(\sigma, V)$ of (19) will force

$$\Delta E[\sigma, V(x_1)] \neq \Delta E[\sigma, V(x_2)]$$

hence the equilibrium condition will shift to $x_1'$ and $x_2'$, altering the shape of the phase diagram. A few examples are noteworthy:

(i) While, as stated above, order–disorder phenomena at fixed composition depend but on $\{\epsilon^{(n)}\}$, the formation enthalpy $\Delta H^{(n)}$ of an ordered phase depends on the *balance* between the "chemical" energy $\epsilon^{(n)}$ and the elastic energy $G(X_n)$ [equation (19)]. Fitting the observed critical temperatures in $\epsilon$-only Ising models [18] will hence inevitably result in erroneous enthalpies. Conversely, fitting $\epsilon^{(n)}$ to be the observed formation enthalpy will result in erroneous critical temperatures. Indeed, interpreting $\epsilon^{(2)} = -5.3$ kcal/g-atom obtained by Kikuchi *et al.* [18] from fitting the critical temperatures for Cu–Au to be the formation enthalpy $\Delta H^{(2)}$ [since by (16) $\Delta H(n) = \epsilon(n)$ if $\Delta F = 0$], one finds a remarkable conflict with the observed [17] $\Delta H^{(2)} = -2.1$ kcal/g-atom.

(ii) A number of semiconductor [20] and mineral [29] alloys show a *positive* mixing enthalpy $\Delta H^{D}$ in the disordered (D) phase, yet a *negative* formation enthalpy $\Delta H^{(n)}$ for some of its related ordered structures. Whereas these phenomena are naturally explainable [20, 21] in terms of (13)–(15) [the existence of a *few* clusters $n$ in the disordered phase creates larger elastic energies (hence $\Delta H^{D} > 0$) than in a perfectly ordered phase having but a single cluster type where $\Delta H^{(n)} < 0$ is possible], the $\epsilon$-only models could address this phenomenon only by invoking a generally unmotivated mix of negative and positive $\epsilon$s [29].

(iii) The simultaneous occurrence, in the same phase diagram of size mismatched constituents [21, 30] of a miscibility gap (indicative of ferromagnetic $J$s) and stable ordering (indicative of antiferromagnetic $J$s) is likewise explainable [21] most naturally in terms of equation (15) (antiferromagnetically attractive $\epsilon$s, but positive $\Delta F$ on account of the size mismatch-induced strain), but requires again a postulation of *both* ferromagnetic and antiferromagnetic interactions in the $\epsilon$-only Ising models (e.g. [31]), a postulation which is generally not anchored in the known electronic structure of these systems.

(iv) $\epsilon$-only Ising models have produced unphysically broad single-phase regions and unphysically narrow two-phase regions (in, for example, [18], Cu–Au), whereas inclusion of $\Delta F$ in the Hamiltonian naturally cures this pathology [21].

(v) The phenomenon of *metastable* long-range ordered phases concomitant with a miscibility gap [21] (where the ordered phase has a lower free energy than that of the single-phase disordered system, yet higher than that of the two-phase mixture) is a natural solution [found when $\epsilon^{(n)} < 0$ but $\Delta H^{(n)} = \epsilon^{(n)} + G(X_n) > 0$] to our Ising-like Hamiltonian in which strain is included. No such solutions exist in the nearest-neighbor $\epsilon$-only Hamiltonian.

(vi) The incorporation of elastic effects acts to remove much of the ground state degeneracies characteristic of the $\epsilon$-only Hamiltonian, raising [21] thereby the [19] triple-point temperature (e.g. coexistence of the disordered + AB + $AB_3$ phases) characteristic of the $\epsilon$-only approach.

(vii) The observation of the insolubility of two elemental solids (e.g. Cu–Ag) leads in the $\epsilon$-only model to the inevitable postulation [18] of strong ferromagnetically repulsive $\epsilon$s, in conflict with the fact that first-principles total energy calculations [32] or simple electronegativity-difference arguments predict *negative* chemical energies $\epsilon^{(n)}$ (e.g. $Cu_3Ag$, CuAg and $CuAg_3$). A similar apparent conflict arises when one compares the value of $\epsilon$ deduced from fitting critical temperatures of an A–B phase diagram [18] with the value of the dissociation energy $\epsilon = E[AB] - E[A] - E[B]$ of a diatomic AB molecule [33]. Inclusion of elastic effects explains this effect naturally as a case of $\epsilon^{(n)} < 0$ (antiferromagnetic) but $\Delta F \gg 0$, such that elastic energies limits the solid solubility although at stoichiometric compositions $\epsilon^{(n)} < 0$.

Whereas some of the shortcomings of the $\epsilon$-only Ising model in describing actual phase phenomena could be cured by introducing further neighbor interactions [4], by treating a sufficient number of $\epsilon$s as mathematically-disposable adjustable parameters fit to reproduce some selected phenomenon [18], or by

introducing an *ad hoc* composition dependence into the $\epsilon$s, our fundamental objection remains that such approaches have but a limited informational content in terms of the *physical insights* being gained. In particular, such approaches do not provide a *link* between the electronic structure of the constituents on one hand and the phase stability and phase interconventions which these constituents exhibit when mixed, on the other hand.

We next describe how treating "chemical" ($\epsilon$) and "elastic" $G(x)$ effects on the same footings is both possible and informative.

## 3. TREATING CHEMICAL AND ELASTIC ENERGIES ON THE SAME FOOTINGS

We represent the Cu–Au system at all states of order $\sigma$ as a mixture of five basic tetrahedral clusters $Cu_{4-n}Au_n$ with energy functions $\Delta E(n, V)$. To treat "chemical" and "elastic" interactions on the same footing, and, at the same time establish a link between the phase diagram and the electronic structure we identify these $\Delta E(n, V)$ with the excess energy of *ordered* periodic structures $Cu_{4-n}Au_n$ (the f.c.c. ground state phases [1–4]). While these basic interaction energies could be modelled by various semiclassical approaches [23–27] of the size-mismatch factor, the electrochemical, or the "electronic" factor, we propose at the first stage to compute $\Delta E(n, V)$ self-consistently from first-principles band theory for the corresponding crystals. We use the f.c.c. structures for Cu and Au, the $L1_0$ structure for CuAuI, and the $L1_2$ structure for both $Cu_3Au$ and $CuAu_3$. For each phase we hence calculate, using the local density formalism [34] as implemented in the general-potential linear augmented plane wave method [35] (LAPW) the five functions $\Delta E(n, V)$ for a full range of volumes $V$. Such self-consistent solutions to the band structure and total energy naturally incorporate both "chemical" and "elastic" effects (on the same footing) in a first-principles manner. The resulting excess energy curves for the ordered structures are depicted in Fig. 1; the values at the minima give the equilibrium volumes $V_n$ and formation enthalpies $\Delta H^{(n)}$. Note that $\Delta H^{(n)}$ are negative ($-0.83$, $-1.45$ and $-0.61$ kcal/g-atom for $n = 1$, 2 and 3, respectively), differ considerably from the $\epsilon^{(n)}$ values which fit the phase diagram in an $\epsilon$-only approach [21, 32] ($-3.99$, $-5.27$ and $-3.64$ kcal/g-atom, respectively), and that $\Delta E(n, V)$ show pronounced volume dependences. Nevertheless, the calculated equilibrium properties deviate somewhat from the measured results (e.g. the measured $\Delta H^{(n)}$ values are [17, 36] $-1.71$, $-2.10$ and $\approx -1.4$ kcal/g-atom, and the calculated equilibrium volumes deviate by $\sim 1\%$ from experiment [36]). We return to this point in Section 3.2. The calculated $\Delta E(n, V)$ were fitted for convenience of use to a Murnaghan equation of state [37]. We use these $\{\Delta E(n, V)\}$ as input to solve the

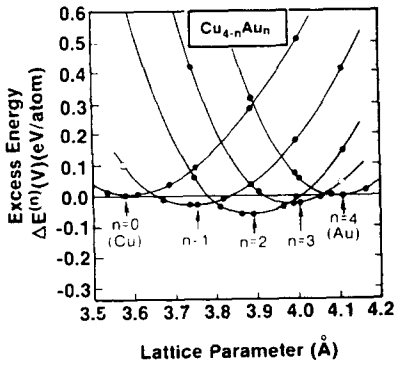


Fig. 1. Calculated excess energies $\Delta E(n, V)$ [equation (11)] for periodic $Cu_{4-n}Au_n$ solids (f.c.c. for $n = 0$ and 4; $L1_0$ for $n = 2$; $L1_2$ for $n = 1$, and 3). Arrows point to the equilibrium lattice parameters.

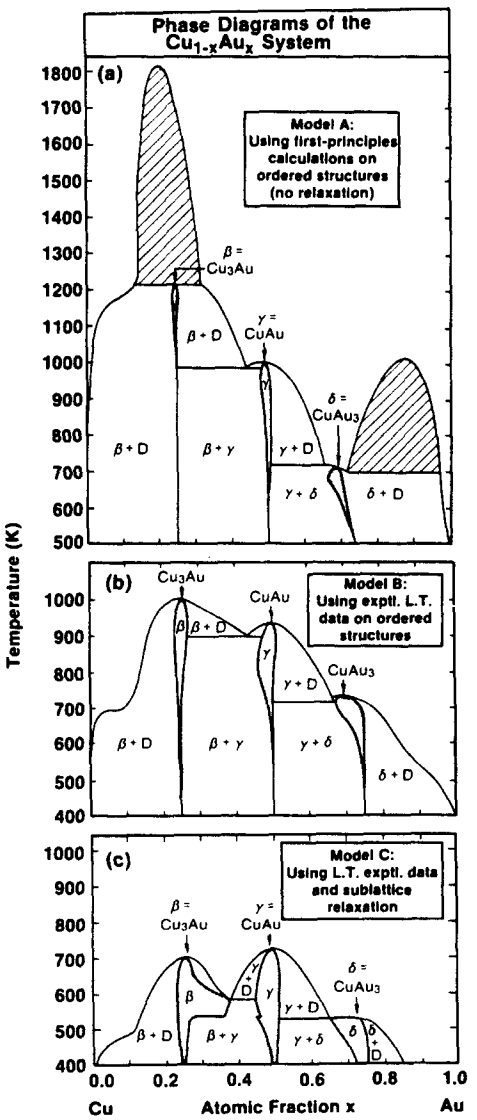


Fig. 2. Calculated phase diagrams for the Cu–Au system in the tetrahedron CVM approach. Model A (Section 3.1); Model B (Section 3.2) and Model C (Section 3.3). Shaded areas denote single phase regions; dashed areas in part (a) denote miscibility gaps.

Ising problem [equations (1)–(8)] within the CVM, retaining a nearest-neighbor four-site physical interaction range and the tetrahedron (topological) counting range. In the CVM calculation we minimize the free energy both with respect to the correlation functions $\xi_n$ *and* with respect to volume.

Note that whereas the notion of extracting alloy interaction parameters from data on ordered crystals is not new [20, 38], their use in Ising models was not attempted previously. In the following three subsections (3.1–3.3) we describe three energy models (denoted as A, B and C, respectively) for calculation of the Cu–Au phase diagrams from $\{\Delta E(n, V)\}$.

### 3.1. Model A: first principles phase diagrams

Using $\{\Delta E(n, V)\}$ of Fig. 1 we calculated the tetrahedron CVM phase diagram of Cu–Au shown in Fig. 2(a) and the excess mixing enthalpies shown for $T = 800$ K in Fig. 3 (by the dotted line), where comparison with the observed [17] mixing enthalpy (solid circles) is also given. The qualitative features of the observed phase diagram [17] are generally reproduced. However, (i) two unobserved miscibility gaps [dashed areas in Fig. 2(a)] are found, (ii) the maximum ordering temperatres are too high, and (iii) the excess mixing enthalpies (Fig. 3) are insufficiently negative.

It is easy to identify the reasons for these quantitative discrepancies with experiment: the phase diagram exhibits an extreme sensitivity to the details of the elastic energies (neglected altogether by previous approaches), and even rather modest discrepancies between the predicted equilibrium properties $\{\Delta H^{(n)}, V_n, B_n\}$ of the *ordered* phases and experiment are amplified into substantial discrepancies in the *phase diagram*.

The next logical step is to study the extent to which errors in the description of the five *ordered phases* $Cu_{4-n}Au_n$ affect the order–disorder and two-phase equilibria.

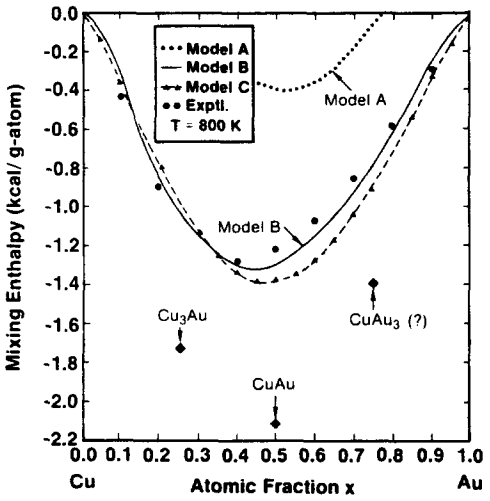


Fig. 3. Calculated and measured [17] excess mixing enthalpy of $Cu_{1-x}Au_x$ at 800 K. The diamond shaped symbols indicate the observed formation enthalpies of the ordered phases.

### 3.2. Model B: using the low-temperature experimental data for ordered compounds

Instead of evaluating our Murnaghan fits to $\Delta E(n, V)$ using the first-principles *calculated* constants $\{\Delta H^{(n)}, V_n, B_n\}$ of the ordered phases, we replace these constants by the *observed* [17, 36] low-temperature values for the same ordered phases, and recalculate the CVM phase diagram. The objective of this model is to appraise the extent to which *five ordered stoichiometric structures* characterized by "perfectly known" structural constants (at low $T$) can reproduce the phase diagram at all temperatures and compositions. Note that the largest change between model A and model B is but 0.04 Å in equilibrium lattice constants and 0.9 kcal/g-atom in the formation enthalpy. The resulting phase diagram is shown in Fig. 2(b) and the mixing enthalpy is given by the solid line in Fig. 3.

These results show (i) the spurious miscibility gaps of model A have disappeared, (ii) the mixing enthalpies are in nearly perfect agreement with experiment (e.g. at $T = 800$ K the calculated values at $x = 1/4$, 1/2 and 3/4 are $-1.01$, $-1.31$ and $-0.79$ kcal/g-atom compared with the measured values [17] of $-1.06$, $-1.22$ and $-0.72$ kcal/g-atom, respectively); (iii) Unlike the $\epsilon$-only phase diagram of Kikuchi *et al.* [18], the single-phase regions [shaded areas in Fig. 2(b)] are narrow and the two-phase regions (clear areas) are broad, and (iv) the critical order/disorder temperatures are closer to experiments. Note that since CVM overestimates critical temperatures with respect to more accurate solutions (e.g. Monte-Carlo, or MC) to the *same* Hamiltonian (by $T_{MC}/T_{CVM} \approx 0.9425$; see Ref. [5]), one should multiply the CVM temperatures by 0.9425 [5, 12, 19] before comparing with experiment. This yields for model B $T_1 = 942.5$ K, $T_2 = 886$ K and $T_3 = 697.5$ K for the order–disorder transitions at $x = 1/4$, 1/2 and 3/4, respectively, compared with the observed values [17] 662, 683 and $\sim 500$ K, respectively.

We conclude that the *remaining* discrepancies between model B and experiment are largely associated with *inherent* physical deficiencies in using but five *ideal* clusters. This is treated next in model C.

### 3.3. Model C: including lattice relaxations

Unlike the phenomenological approaches which fit the phase diagram, the present approach offers the opportunity to analyze *failures* in terms of discernible physical factors left out from the model. For example, both models A and B tacitly assumed that the equilibrium volumes $V_n$ of the ordered clusters $Cu_{4-n}Au_n$ (each embedded in an environment of *identical* clusters in the perfectly ordered phases) can be used to represent the alloy at all compositions $x$ (where different cluster types can coexist). In reality, one expects that the elastic energy of the system

can be reduced if the *equilibrium* molar volumes $V_n$ of each cluster will relax (differently for each composition $x$) to better accommodate the volume mismatch. Hence, the variation of the equilibrium volumes of the $Cu_{4-n}Au_n$ clusters in the alloy $Cu_{1-x}Au_x$ can be described by a general Taylor expansion of the form

$$V_n(x) = V_n(X_n) + K_n[V(x) - V_n(X_n)] + \cdots, \quad (21)$$

where $V_n(X_n)$ is the equilibrium volume of the stoichiometric composition $X_n = n/4$ of the ordered phase. $V(x)$ is the alloy volume and $\{K_n\}$ are some relaxation constants. In the harmonic elastic regime, these relaxations alter the excess energies by

$$\Delta E[n, V(x)] = \Delta H^{(n)} + \frac{B_n}{2V_n}(1 - K_n)^2 \times [V(x) - V_n(X_n)]^2 + \cdots. \quad (22)$$

Note that $K_n = 0$ corresponds to the unrelaxed limit of models A and B where $V_n(x) = V_n(X_n)$ for all $x$ (analogous to the classical notion of Bragg [39] and Pauling [28] that to first order atoms retain their specific radii in different chemical environment, including different compositions $x \neq X_n$), whereas $K_n = 1$ corresponds to the "virtual lattice model", where all distinct $V_n$s average in the alloy to a single $V_n(x) = V(x)$, independent of $n$.

Rather than seek a *set* of $n$-dependent relaxation parameters $\{K_n\}$, we pose instead the following question: does there exist a *single* effective relaxation parameter $K$ which when applied equally to the equilibrium volumes $V_n(x)$ of the five actual ordered phases [equation (21)], cures all of the discrepancies of the calculated phase diagram of model B relative to experiment?

Model *C* answers that question by seeking just such a relaxation constant. We find $K = 0.2077$ for Cu–Au (i.e. Paulings view is only about 20% wrong whereas the virtual lattice model is ~80% wrong). The resulting phase diagram is shown in Fig. 2(c), and the mixing enthalpies are given in Fig. 3 by the solid triangles. The critical temperatures agree with experiment [17] to within ~1 K, and the mixing enthalpies deviate by less than <0.1 kcal/g-atom. The calculated partial molar enthalpies of solutions at 800 K [given by Lim $\Delta H(x, T)/x(1-x)$ at $x \to 0$ or $x \to 1$, a numerically highly-sensitive quantity] are −2.35 kcal/g-atom for Au dissolved in Cu and −3.1 kcal/g-atom for Cu dissolved in Au, compared with the observed values [17] of −3.9 and −2.8 kcal/g-atom, respectively. (In the absence of relaxation the partial molar enthalpies are *positive*, in qualitative conflict with experiment, whereas if strain energies are neglected altogether [18], these quantities are substantially too negative.) The diamond-shaped symbols in Fig. 3 show the formation enthalpies of the three *ordered* phases, demonstrating (as argued before [20]) that they are invariably lower than the corresponding mixing enthalpies of the disordered phase. Figure 4 shows the normalized excess enthalpy $[\Omega_H = \Delta H/x(1-x)]$, entropy $[\Omega_S = \Delta S/x(1-x)]$ and free energy $[\Omega_F = \Delta F/x(1-x)]$ at three temperatures, demonstrating (i) a negative excess entropy, in conflict with earlier data [17] but in agreement with more accurate recent data [40] and (ii) strong short-range order-induced deviations of all $\Omega$ from linearity. [It is important to note that the $\epsilon$-only model [18], fit to critical temperatures produces [21] enormous errors in the mixing enthalpies and partial molar enthalpies (too negative by ~400% at $T = 800$ K), clearly due to the neglect of elastic effects], and (iii) a reduction in the composition variation of all $\Omega$ at high temperatures.

As indicated above, in our CVM calculation we minimize simultaneously the free energy with respect to probabilities *and* the volume. This provides the predicted volume (or lattice parameter) function $V(x, T)$ for each phase. In Figs 5(a–c) we present the behavior of the lattice parameter for compositions $x = 0.25$, 0.50, 0.75 near their transition temperatures. In the three cases there is a discontinuity when one passes the phase transition region. The discontinuity is larger for $Cu_3Au$ [Fig. 5(a)] and smaller for $CuAu_3$ [Fig. 5(c)]. While we find the transition region for $Cu_3Au$ to be very narrow [less than 0.1 K, see Fig. 5(a)], for $CuAu_3$ [Fig. 5(c)] the transition region (shaded area) extends in a range of almost 40 K. The discontinuities for CuAu and

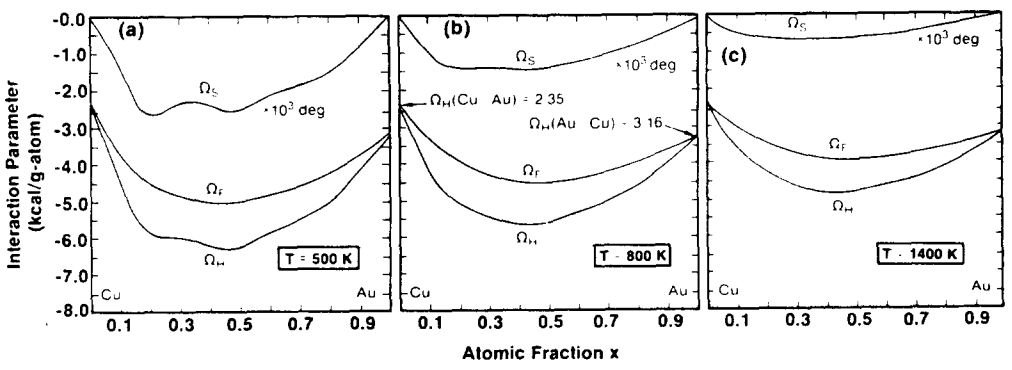


Fig. 4. Calculated normalized excess thermodynamic functions for Cu–Au in Model C. $\Omega_S = \Delta S/x(1-x)$; $\Omega_H = \Delta H/x(1-x)$; $\Omega_F = \Delta F/x(1-x)$.

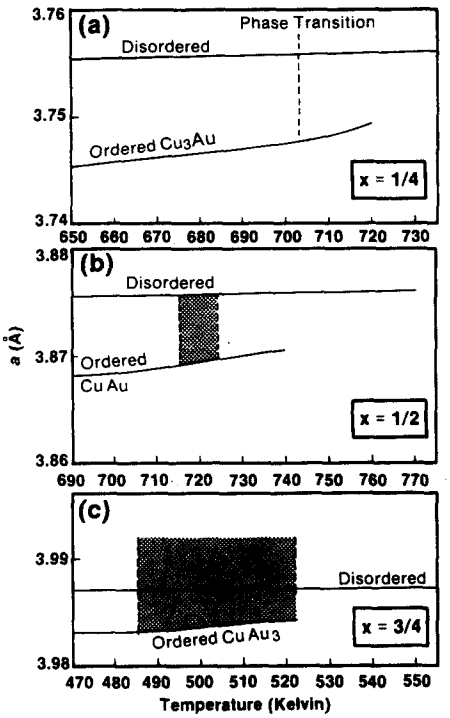


Fig. 5. Temperature variation of the equilibrium lattice parameters as calculated from model C. Shaded areas denote the phase transition regions.

$CuAu_3$ are diffiicult to observe experimentally because, in the case of CuAu there is a tetragonal distortion when crossing to the ordered phase while, for $CuAu_3$, the transition region is so broad and the volume discontinuity so small that it is unlikely that the internal strains could prevent the formation of multiphase domains. On the other hand the discontinuity of $Cu_3Au$ has been observed to be some thousandths of Ångstroms, while our calculated result is 0.0080 Å, in reasonable agreement with experiment [41].

We concluded that the phase diagram of a lattice-mismatched system such as Cu–Au can be reproduced by treating "chemical" and "elastic" energies simultaneously and accounting for lattice relaxation. Neglect of the elastic energy [18] and relaxation produces but the order–disorder critical temperatures while (i) overestimating greatly both the formation enthalpies of the ordered phases and the mixing enthalpies of the disordered phase, (ii) greatly overestimating (understimating) the regions of single-phase (two-phase coexistence). Extension of this work to include the Cu–Ag and Ag–Au systems will be published in the future [32].

## 4. CONCLUSONS

Our results can be summarized as follows:

(i) Attempts to cure the systematic deviation from experiment of the phase diagrams calculated within the nearest-neighbor generalized Ising model by improving on the topological counting range (say, beyond tetrahedron) or on counting algorithms, have solved only part of the problem. The reason for the failures is physical (not statistical) and involve the neglect of (long-range) forces which are not representable through *any* set of fixed-interaction energies $\{\epsilon^{(n)}\}$.

(ii) The inclusion of "elastic" effects [or any other long-range effects attendant upon first-principles calculations of $\Delta E(n, V)$] involves merely a *reinterpretation* of the coupling constants in light of our two-step conceptual model (Section 1) which clarifies their *physically mandated* volume-dependence.

(iii) The use of structural and elastic low-temperature data on only five (ground state) ordered phases suffices to obtain *semi-quantitative* phase diagrams and quantitative excess thermodynamic functions over the entire temperature and composition range, if sufficient accuracy in the input data ($\sim 0.5\%$ for lattice parameters, $\sim 8\%$ in formation enthalpies) is available. State-of-the-art first principles calculations on ordered phases yet lack this high degree of accuracy.

(iv) *Quantitative* reproduction of phase diagrams for lattice-mismatched constituents requires ($\sim 20\%$) lattice relaxation which acts to better accommodate elastically local clusters of different sizes.

## REFERENCES

1. C. Domb, in *Phase Transitions and Critical Phenomena* (Edied by C. Domb and H. S. Green), Vol. 3, p. 357. Academic Press, London (1974).
2. D. M. Burley, in *Phase Transitions and Critical Phenomena* (Edited by C. Domb and H. S. Green), Vol. 2, p. 329. Academic Press, London (1972).
3. L. H. Bennett (Editor), *Theory of Alloy Phase Formation*. The Metallurgical Society, Warrendale, Pa. (1980).
4. D. DeFontaine, in *Solid State Physics* (Edited by H. Ehrenreich, F. Seitz and D. Turnbull), Vol. 37, p. 73. Academic Press, New York (1979).
5. D. F. Styer, M. K. Phani and J. Lebowitz, *Phys. Rev.* **B34,** 3361 (1986).
6. W. Shockley, *J. Chem. Phys.* **6,** 130 (1938).
7. W. L. Bragg and E. J. Williams, *Proc. R. Soc.* **A145,** 699 (1934).
8. H. A. Bethe, *Proc. R. Soc.* **A150,** 552 (1935).
9. E. A. Guggenheim, *Proc. R. Soc.* **A169,** 134 (1938).
10. Y. Y. Li, *J. Chem. Phys.* **17,** 447 (1949).
11. Y. Takagi, *Proc. Phys. Math. Soc. Jap.* **23,** 44 (1941).
12. C. M. van Baal, *Physica* **64,** 571 (1973).
13. R. Kikuchi, *J. Chem. Phys.* **60,** 1071 (1974).
14. N. S. Golosov, L. E. Popov and L. Yu. Pudan, *J. Chem. Phys. Solids* **34,** 1149, 1157 (1973).
15. J. M. Sanchez and D. de Fontaine, *Phys. Rev.* **B21,** 216 (1980).
16. J. M. Sanchez and D. de Fontaine, *Phys. Rev.* **B17,** 2926 (1978).
17. See compilation of data by R. Hultgren, R. D. Desai, D. T. Hawkins, H. G. Gleiser and K. K. Kelley in *Selected Values of the Thermodynamic Properties of Binary Alloys*. American Society for Metals, Cleveland (1973).
18. R. Kikuchi, J. M. Sanchez, D. de Fontaine and H. Yamaguchi, *Acta metall.* **28,** 651 (1980); D. de Fontaine and R. Kikuchi, NBS report SP-496, p. 967 (1977).

19. K. Binder, *Phys. Rev. Lett.* **45,** 811 (1980); U. Gahn, *J. Phys. Chem. Solids* **47,** 1153 (1986 ); A. Finel and F. Ducastelle, *Europhys. Lett.* **1,** 135, 543/E (1986).
20. G. P. Srivastava, J. L. Martins and A. Zunger, *Phys. Rev.* **B31,** 2561 (1985).
21. L. G. Ferreira, A. A. Mbaye and A. Zunger, *Phys. Rev.* **B35,** 6475 (1987); A. A. Mbaye, L. G. Ferreira and A. Zunger, *Phys. Rev. Lett.* **58,** 49 (1987).
22. For earlier accounts on the role of elastic energies on the phase diagram see, for example, J. W. Cahn, *Acta metall.* **9,** 795 (1961), *ibid.* **10,** 179 (1962); A. G. Khachaturyan, *Sov. Phys. Solid State* **5,** 16 (1963); D. deFontaine, *Acta metall.* **21,** 553 (1973); T. Kajitani and H. Cook, *Acta metall.* **26,** 1371 (1978); H. E. Cook, *Acta metall.* **21,** 1431 (1973); H. Kubo, *Phys. Rev.* **B32,** 4687 (1985); A. Bieber and F. Gautier, *Acta metall.* **35,** 1839 (1987).
23. W. B. Pearson, *The Crystal Chemistry and Physics of Metal Alloys.* Wiley Interscience, New York (1972).
24. E. Mooser and W. B. Pearson, *Acta crystallogr* **12,** 1015 (1954).
25. A. Zunger, *Phys. Rev. Lett.* **44,** 582 (1980); *ibid. Phys. Rev.* **B22,** 5839 (1980).
26. L. S. Darken and R. W. Gurry, *Physical Chemistry of Metals.* McGraw-Hill, New York (1953).
27. A. R. Miedema, R. Boom and F. R. deBoer and J. Less. *Common Met.* **40,** 283 (1975).
28. L. Pauling, *The Nature of the Chemical Bond.* Cornell University Press, Ithaca, New York (1960).
29. C. Capobianco, B. Burton, P. M. Davidson and A. Navrotsky, *J. Solid State Chem.* They find a *negative* formation enthalpy for ordered $CdMg(CO_3)_2$ but a *positive* mixing enthalpy for the disordered phase.
30. See D. E. Laughlin, K. B. Alexander and L. L. Lee, in *Decomposition of Alloys: The Early Stages* (Edited by P. Haasen, V. Gerold, R. Wagner and M. F. Ashby), Pergamon Press, Oxford (1984) for a review of concomitant ordering and immiscibility in metal alloys. An analogous effect was recently observed in semiconductors by H. R. Jen, M. J. Cherng and G. B. Stringfellow, *Appl. Phys. Lett.* **48,** 1603 (1986).
31. S. M. Allen and J. W. Cahn, *Acta metall.* **24,** 425 (1976).
32. S. H. Wei, A. A. Mbaye, L. G. Ferreira and A. Zunger *Phys. Rev.* **B36,** 4163 (1987). We have noted in this work that small errors in the calculated total energies are amplified into large changes in the phase diagram. In particular, using approximate total energy methods [e.g. the Augmented Spherical Waves method of K. Terakura, T. Oguchi, T. Mohri and K. Watanabe, *Phys. Rev.* **B35,** 2169 (1986)] may lead to superficially better phase diagrams even if relaxation is ignored.
33. K. P. Huber and G. Herzberg, *Molecular Spectra and Molecular Structure Constants of Diatomic Molecules.* Van Nostrand, New York (1979) give the following molecular disociation energies (in eV) $Ag_2$ (1.66); $Cu_2$ (2.03); $Au_2$ (2.30); AgCu (1.76); AgAu (2.06), and CuAu (2.36).
34. P. Hohenberg and W. Kohn, *Phys. Rev.* **136,** 864 (1964); W. Kohn and L. J. Sham, *Phys. Rev.* **140,** 1133 (1965).
35. S.-H. Wei, H. Krakauer and M. Weinret, *Phys. Rev.* **B32,** 7792 (1985) and references therein.
36. *Landolt-Börnstein New Series* 6. Springer, Berlin (1971).
37. F. D. Murnaghan, *Proc. natn. Acad. Sci. U.S.A.* **30,** 244 (1944).
38. J. W. D. Connolly and A. R. Williams, *Phys. Rev.* **B27,** 5169 (1983).
39. W. L. Bragg, *Phil. Mag.* **40,** 169 (1920).
40. L. Topor and O. J. Kleppa, *Metall. Trans.* **15A,** 2 (1984); O. J. Kleppa and L. Topor in *Noble Metal Alloys* (Edited by T. B. Massalski, W. B. Pearson, L. H. Bennett and Y. A. Chang), p. 199. The Metallurgical Society, Warrendale, Pa (1980).
41. H. L. Yakel, *J. appl. Phys.* **33,** 2439 (1962).